

Keywords: gastric cancer; EpCAM; BerEP4; EpICD; PSEN2; ADAM17

Members of the EpCAM signalling pathway are expressed in gastric cancer tissue and are correlated with patient prognosis

V S Warneke¹, H-M Behrens¹, J Haag¹, S Krüger¹, E Simon¹, M Mathiak¹, M P A Ebert² and C Röcken^{*1}

¹Department of Pathology, Christian-Albrechts-University, Arnold-Heller-Strasse, D-24105 Kiel, Germany and ²Faculty of Clinical Medicine Mannheim, Department of Medicine II, University of Heidelberg, Mannheim, Germany

Background: We investigated the expression of members of the epithelial cell adhesion molecule (EpCAM) signalling pathway in gastric cancer (GC) testing the following hypotheses: are these molecules expressed in GC and are they putatively involved in GC biology.

Methods: The study cohort consisted of 482 patients. The following members of the EpCAM signalling pathway were analysed by immunohistochemistry and were correlated with various clinico-pathological patient characteristics: extracellular domain of EpCAM (EpEX), intracellular domain of EpCAM (EpICD), E-cadherin, β -catenin, presenilin-2 (PSEN2), and ADAM17.

Results: All members of the EpCAM signalling pathway were differentially expressed in GC. The expression correlated significantly with tumour type (EpEX, EpICD, E-cadherin, β -catenin, and PSEN2), mucin phenotype (EpEX, EpICD, β -catenin, and ADAM17), T-category (EpEX, E-cadherin, and β -catenin), N-category (EpEX and β -catenin), UICC tumour stage (EpEX, EpICD, β -catenin, and PSEN2), tumour grade (EpEX, EpICD, E-cadherin, β -catenin, and PSEN2), and patients' survival (EpEX, EpICD, and PSEN2). A significant coincidental expression in GC was found for EpEX, EpICD, E-cadherin, β -catenin, PSEN2, and ADAM17. Decreased immunodetection of EpEX in locally advanced GC was not associated with decreased EpCAM mRNA levels.

Conclusion: All members of the EpCAM signalling pathway are expressed in GC. The expression correlated significantly with each other and with various clinico-pathological patient characteristics, including patients' survival. Thus, the EpCAM signalling pathway is a highly interesting putative therapeutic target in GC.

In recent decades we witnessed major advancements in the understanding of the epidemiology, pathology, and pathogenesis of gastric cancer (GC). Infection with *H. pylori* or Epstein–Barr virus, and dietary and lifestyle factors contribute to the risk of developing GC. These advancements were accompanied by the introduction of chemotherapy for the treatment of GC, which is evolving continuously and improves patients' survival (Alberts *et al*, 2003; Cunningham *et al*, 2006; Paoletti *et al*, 2010). Evidence is increasing that patient prognosis and treatment response does not only depend on tumour stage but also on the expression and tumour-specific alteration of signalling pathways. A target

currently explored in GC is the epithelial cell adhesion molecule (EpCAM; CD326). The US National Institute of Health (www.clinicaltrials.gov) currently lists five studies investigating drugs targeting EpCAM, such as catumaxomab and MT110. Catumaxomab and MT110 are bispecific antibodies, which bind to EpCAM and CD3.

Maetzel *et al* (2009) recently provided evidence that regulated intramembrane proteolysis (RIP) activates EpCAM as a mitogenic signal transducer *in vitro* and *in vivo*. This involves shedding of the ectodomain extracellular domain of EpCAM (EpEX) and nuclear translocation of the intracellular domain of EpCAM (EpICD).

*Correspondence: Professor Dr C Röcken; E-mail: christoph.roecken@uk-sh.de

Received 24 February 2013; revised 4 August 2013; accepted 14 August 2013; published online 5 September 2013

© 2013 Cancer Research UK. All rights reserved 0007–0920/13

Cleavage of EpCAM is sequentially catalysed by ADAM17 and presenilin-2 (PSEN2). Released EpICD associates with FHL2, β -catenin, and Lef-1 to form a nuclear protein complex, leading to gene transcription (Maetzel *et al.*, 2009; Figure 1). However, currently, there is no evidence to suggest that RIP-mediated cell signalling of EpCAM may also apply to GC. Here we wished to fill this gap of information by systematically investigating the expression of members of the EpCAM signalling pathway, that is, EpCAM, E-cadherin, β -catenin, PSEN2, and ADAM17, in GC testing the following hypotheses: are these molecules expressed in GC and are they putatively involved in GC biology.

MATERIALS AND METHODS

Ethics statement. This project was approved by the local ethics committee of the University Hospital in Kiel, Germany (reference number D 453/10). All patient data were pseudonymised before study inclusion.

Study population. From the archive of the Institute of Pathology, University Hospital Kiel, we identified all Caucasian patients who had undergone either total or partial gastrectomy for adenocarcinomas of the stomach or the oesophago-gastric junction between 1997 and 2009 (GC cohort). The following patient characteristics were retrieved: type of surgery, age at diagnosis, gender, tumour localisation and tumour size, tumour type, tumour grade, depth of invasion, number of lymph nodes resected, and number of lymph nodes with metastases. Date of patient death was obtained from the Epidemiological Cancer Registry of the state of Schleswig-Holstein, Germany. Follow-up data of patients still alive were retrieved from hospital records and from general practitioners (Supplementary Table 1). Unfixed, fresh frozen malignant and corresponding non-

malignant tissues were available from 55 of these patients, to study mRNA expression (Supplementary Table 2).

A cohort of 30 consecutive sleeve gastrectomy specimens operated in 2012 and 2013 at the University Hospital Kiel was retrieved from the archive (sleeve gastrectomy cohort). Study inclusion criteria were no evidence of any gastric neoplasia. The mean age of the patients was 39 years (range 20–66 years), including 16 women and 14 men.

Study inclusion and exclusion criteria. Inclusion and exclusion criteria for the GC cohort were defined as follows: patients were included when (1) histology confirmed an adenocarcinoma of the stomach or the oesophago-gastric junction, and (2) the date of death or survival data were available. Patients were excluded when (1) histology identified a tumour type other than adenocarcinoma, (2) histopathological data were incomplete, (3) patients had previously undergone a resection of a Billroth-II stomach with cancer in the gastric remnant, and (4) date of patient death or survival data had not been recorded. Patients who received perioperative chemotherapy were also excluded.

Histology and TNM classification. Tissue specimens were fixed in formalin and embedded in paraffin. Deparaffinised sections were stained with haematoxylin and eosin. Tumours were classified according to the Laurén classification (Lauren, 1965) and the mucin phenotype (Namikawa and Hanazaki, 2010). All cases included in this study were re-examined by two surgical pathologists (VW, CR). pTNM stage of all study patients was determined according to the seventh edition of the UICC guidelines (Sobin *et al.*, 2009) and our recent proposal ('Kiel stage'; Warneke *et al.*, 2011), and was based solely on surgical pathological examination, including classification of distant metastases (pM category). In the seventh edition, all tumours of the oesophago-gastric junction and tumours of the proximal 5 cm of the stomach with extension into the oesophagus are classified as oesophageal tumours (Sobin *et al.*, 2009). Patients were re-categorised accordingly.

Tissue micro array construction. Formalin-fixed and paraffin-embedded (FFPE) tissue samples were used to generate tissue micro arrays (TMAs) as described previously (Weichert *et al.*, 2008). Three morphologically representative regions of the paraffin 'donor' blocks were chosen. Tissue cylinders of 1.5 mm diameter were punched from these areas and were precisely arrayed into a new 'recipient' paraffin block. Two-micrometre sections of the TMA blocks were cut for further analysis.

Cell culture. The human GC cell line MKN74 was obtained from the Japanese Health Science Research Resource Bank (Osaka, Japan) and HEK293 EBNA cells were purchased from Invitrogen (Carlsbad, CA, USA). The cells were grown in RPMI 1640 medium (MKN74) or Dulbecco's modified Eagle medium (HEK293) supplemented with 10% fetal bovine serum, 100 U ml⁻¹ penicillin and 100 μ g ml⁻¹ streptomycin (PAA Laboratories GmbH, Pasching, Austria).

Western blotting. The specificity of the anti-PSEN2-antibody used for immunostaining (EP1515Y; Abcam, Cambridge, UK) was tested using a PSEN2 overexpression lysate created in HEK cells and the empty vector negative control (HEK293 cell lysate; Novus Biologicals; Littleton, CA, USA). In addition, protein lysates were obtained by incubating human GC tissue and cultured cells with RIPA buffer (50 mM Tris-HCl pH 7.6, 150 mM NaCl, 1% NP-40, 0.5% sodium deoxycholate, 0.2% SDS) and protease inhibitor cocktail (Complete EDTA-free; Roche Diagnostics, Mannheim, Germany). Protein samples were denatured in Laemmli buffer (60 mM Tris-HCl pH 6.8, 2% SDS, 10% glycerol, 5% β -mercaptoethanol, and 0.01% bromophenol blue) by heating at 95 °C for 10 min, and were subsequently loaded on 4–15%

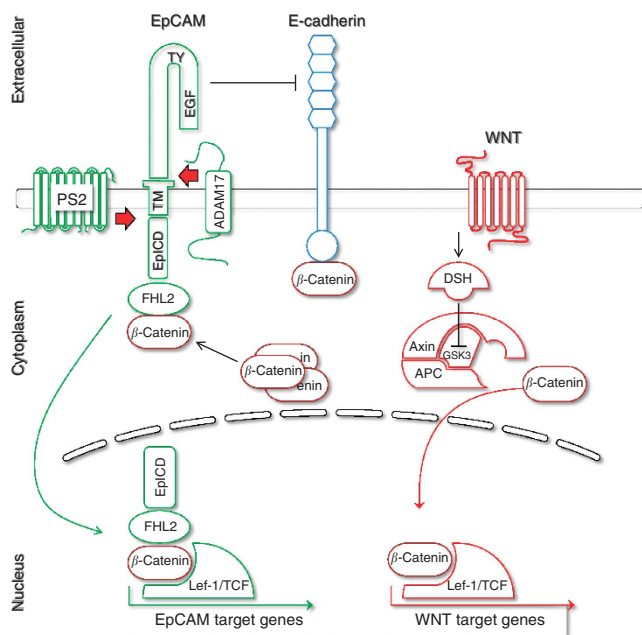


Figure 1. EpCAM and WNT signalling pathways. A regulated intramembrane proteolysis (RIP) involves shedding of the ectodomain EpEX and nuclear translocation of the intracellular domain EpICD. Cleavage of EpCAM is sequentially catalysed by ADAM17 and PSEN2. Released EpICD associates with FHL2, β -catenin, and Lef-1 to form a nuclear protein complex, leading to gene transcription (modified from Maetzel *et al.* (2009)).

Mini-PROTEAN TGX Precast Gel (Bio-Rad; Munich, Germany) and visualised by staining with Coomassie blue. After separation, proteins on unstained polyacrylamide gels were transferred to a PVDF membrane (Macherey-Nagel, Düren, Germany), immunoblotted with the anti-PSEN2-antibody (dilution 1:500) and an anti- β -actin-antibody (1:10 000, clone AC-15; Sigma Aldrich, Munich, Germany) to ensure equal loading amounts. Membrane-bound HRP-labelled secondary antibodies (dilution 1:2000; DakoCytomation, Glostrup, Denmark) were detected by enhanced chemiluminescence using the ECL system (GE Healthcare Life Sciences, Freiburg, Germany). Omission of the primary antibody served as a negative control.

Immunohistochemistry. Immunohistochemistry was carried out with monoclonal antibodies directed against mucin 1 (clone MA695; dilution 1:100) and mucin 2 (clone Ccp58; both from Novocastra, Leica Microsystems GmbH, Wetzlar, Germany; 1:100); mucin 5 (clone 45M1; Thermo Scientific, Schwerte, Germany; 1:100); mucin 6 (clone CLH5; 1:100) and CD10 (clone 56C6; both from Novocastra; 1:10); E-cadherin (clone SPM471; ZYTOMED Systems GmbH, Berlin, Germany; 1:400); β -catenin (clone Cat-5H10; Life Technologies GmbH, Darmstadt, Germany; 1:300); EpEX (clone Berep4; Dako Deutschland GmbH, Hamburg, Germany; 1:500); EpICD (clone E144; Biomol, Hamburg, Germany; 1:100); PSEN2 (dilution 1:50) and MLH1 (clone G168-15; BD Biosciences, Heidelberg, Germany; 1:50); PMS2 (clone MRQ-28; Cell Marque Corporation, Rocklin, CA, USA; 1:20); MSH2 (clone FE11; Calbiochem, Merck KGaA, Darmstadt, Germany; 1:30); MSH6 (clone 44; BD Biosciences; dilution 1:30); and a polyclonal antibody directed against ADAM17 (Sigma Aldrich; dilution 1:200).

Antigen retrieval was performed manually with 10 mM citrate buffer (pH 6.0) in a pressure cooker at 120 °C for 10 min (PSEN2 and ADAM17) or in TEC buffer (Tris-EDTA-Citrate pH 7.8) using the DakoCytomation Pascal pressure chamber (DakoCytomation; Hamburg, Germany) at 125 °C for 1 min (MLH1, MSH2, and MSH6), respectively. Automated antigen retrieval was performed in ER1 (citrate buffer Bond pH 6.0; mucin 1, and CD10), or in Ultra-CC1 (Tris-based buffer from Ventana (Ventana Medical Systems, Tucson, AZ, USA) with a slightly basic pH; EpICD), ER2 (EDTA-buffer Bond pH 8.9; mucin 2, mucin 6, E-cadherin, β -catenin, and PMS2) or with Enz1 (Protease Bond; EpEX) according to the manufacturer's instructions and using the autostainer Bond Max System (Leica-Menarini, Berlin, Germany) or for EpICD the autostainer Benchmark ULTRA (Ventana Medical Systems). Immunostaining was done with the Bond Max System (mucin 1 to 6, CD10, E-cadherin, β -catenin, EpEx, and PMS2) using the Bond Polymer Refine Detection Kit (Leica-Menarini) or with the Benchmark ULTRA (Ventana Medical Systems; EpICD) using the ULTRAVIEW Universal DAB Detection Kit (Ventana Medical Systems). Immunostaining of ADAM17, PSEN2, MSH6, MSH2, and MLH1 was performed manually. After a blocking step with Hydrogen Peroxide Block (Thermo Scientific; PSEN2, MSH6, MSH2, and MLH1), the samples were incubated with the respective antibodies at 4 °C overnight and the immunoreaction was visualised with the Histofine simple stain MAX PO Multi detection reagent (Nichirei Biosciences Inc., Tokyo, Japan) in combination with the DAB Peroxidase Substrate Kit (Vector Laboratories Inc., Burlingame, CA, USA; PSEN2, MSH6, MSH2, and MLH1) or with the UltraVision Large Volume Detection System anti-Rabbit AP (Thermo Scientific; ADAM17) and the SIGMAFAST Fast Red TR/Naphthol AS-MX Tablets (Sigma Aldrich) according to the manufacturer's instructions. Counterstaining was done with haematoxylin (Dr K Hollborn & Söhne GmbH & Co KG, Leipzig, Germany).

The specificity of the immunostaining was verified by using positive controls recommended by the manufacturers, participation in external quality assurance programmes (see below), by omission of the primary antibody (all antibodies) and by western blotting (PSEN2; see Supplementary Figure 1).

External quality assurance. The immunohistochemical evaluation of DNA mismatch repair proteins (MSH2, MSH6, MLH1, and PMS2) was certified successfully by the quality assurance programme of the German Society of Pathology and the Bundesverband Deutscher Pathologen e.V.

Evaluation of immunostaining. Immunostaining of the TMAs was evaluated by applying an immunoreactivity scoring system (IRS). Briefly, category A documented the intensity of

Table 1. Clinico-pathological patient characteristics of the GC cohort

Patient characteristics			
Patients		(n)	482
Age (years)		Mean \pm s.d. Median	67.9 \pm 11.1 68
Gender	Men Women	(n (%)) (n (%))	297 (61.6) 185 (38.4)
Follow-up data	Alive Dead	(n (%)) (n (%))	131 (28.1) 335 (71.9)
Localisation	Proximal Distal	(n (%)) (n (%))	149 (30.9) 333 (69.1)
pT-category	pT1a pT1b pT2 pT3 pT4a pT4b	(n (%)) (n (%)) (n (%)) (n (%)) (n (%)) (n (%))	13 (2.7) 49 (10.2) 56 (11.6) 190 (39.4) 134 (27.8) 40 (8.3)
pN-category	pN0 pN1 pN2 pN3/a/b	(n (%)) (n (%)) (n (%)) (n (%))	138 (28.8) 67 (14.0) 85 (17.7) 189 (39.5)
UICC Stage (7th edn)	IA IB IIA IIB IIIA IIIB IIIC IV	(n (%)) (n (%)) (n (%)) (n (%)) (n (%)) (n (%)) (n (%)) (n (%))	49 (10.4) 32 (6.8) 58 (12.3) 47 (9.9) 55 (11.6) 83 (17.5) 66 (14.0) 83 (17.5)
Stage according to Kiel proposal	I II IIIA IIIB IV	(n (%)) (n (%)) (n (%)) (n (%)) (n (%))	49 (10.2) 84 (17.5) 49 (10.2) 153 (31.9) 145 (30.2)
Resected lymph nodes		Mean \pm s.d. Median (n)	19.2 \pm 8.2 18
Positive lymph nodes		Mean \pm s.d. Median (n)	6.4 \pm 7.4 3
LNR		Median (n)	0.2
Tumour grade	G1/G2 G3/G4	(n (%)) (n (%))	111 (23.7) 357 (76.3)
Resection margin (R-status)	R0 R1/R2	(n (%)) (n (%))	403 (88.2) 54 (11.8)
Abbreviations: GC = gastric cancer; LNR = lymph node ratio.			

immunostaining as 0 (no immunostaining), 1 (weak), 2 (moderate), and 3 (strong). Category B documented the percentage of immunoreactive cells as 0 (no immunoreactive cells), 1 (few scattered immunoreactive cells, <1%), 2 (1–10%), 3 (11–50%), 4 (51–80%), and 5 (>80%). The addition of category A and B resulted in an IRS ranging from 0 to 8 for each individual case.

Real-time reverse-transcriptase PCR. Total RNA was isolated from cryoconserved tissues using Ambion's mirVana miRNA Isolation Kit (Applied Biosystems, Darmstadt, Germany) followed by a DNase treatment with Turbo DNA-free kit (Ambion). RNA quality was assessed in a 1.5% agarose gel. For cDNA synthesis, 2 µg of total RNA was reverse transcribed using Maxima First Strand cDNA Synthesis Kit (Thermo Scientific). Gene-specific primers were synthesised by Biomers (Ulm, Germany; see Supplementary Table 3). Real-time reverse-transcriptase PCR (real-time RT-PCR) was carried out using the LightCycler 480 Probes Master (Roche Diagnostics GmbH) and the LightCycler 480 System (Roche Diagnostics GmbH). The comparative Ct values were normalised to that of three housekeeping genes: *Homo sapiens succinate dehydrogenase complex, subunit A, flavoprotein (Fp)*, *Homo sapiens calpain 2*, and *Cyclophilin C*. 'No template' and 'no amplification' controls were run for each gene to detect unspecific or genomic amplification and primer dimerisation. All experiments were performed in duplicates.

DNA isolation. Genomic DNA was extracted from FFPE tissue using the QIAamp DNA mini kit (Qiagen, Hilden, Germany) following the manufacturer's instructions. The integrity and amplifiability of the isolated DNA was evaluated by a qualitative size range PCR assay (van Dongen *et al*, 2003). Tissue sections

were manually microdissected before DNA isolation to enrich for tumour cells (>80%).

Microsatellite instability assay. Microsatellite instability was determined by comparison of the allelic profiles of the mononucleotide repeat markers BAT-25, BAT-26, NR-21, NR-24, and NR-27 in tumour and corresponding normal tissue (Buhard *et al*, 2006). All markers were co-amplified in a pentaplex PCR assay with the QIAGEN Multiplex PCR Master Mix (Qiagen) following the manufacturer's recommendations for amplification of microsatellite loci. The amplified loci were analysed on a 3500 Genetic Analyzer (Applied Biosystems). Samples were judged as microsatellite unstable when the tumour showed instability in at least two of the five (40%) microsatellites analysed.

Statistics. Statistical analyses were performed using SPSS 20.0 (IBM Corporation, Armonch, NY, USA). For continuous variables, cases were divided into two groups by splitting at the median value, except for EpICD, where the marker score distribution suggested splitting into score = 0 (negative) and score > 0 (positive) groups. Median overall survival was determined using the Kaplan–Meier method, and the log-rank test was used to determine significance. For comparison purposes, the median survival time, its s.d., and 95% confidence interval were calculated. To investigate prognostic relevance, we included all variables having $P < 0.10$ into a Cox regression model and used the backward LR method ($P_{in} = 0.05$ and $P_{out} = 0.10$) to reduce the model to the independent variables. The significance of correlation between clinico-pathological parameters and biomarker expressions was tested using Fisher's exact test. For parameters of ordinal scale (T-category, N-category, and tumour stage), we applied Kendall's τ -test instead. Real-time RT-PCR data, which were evaluated with a two-sided Student's

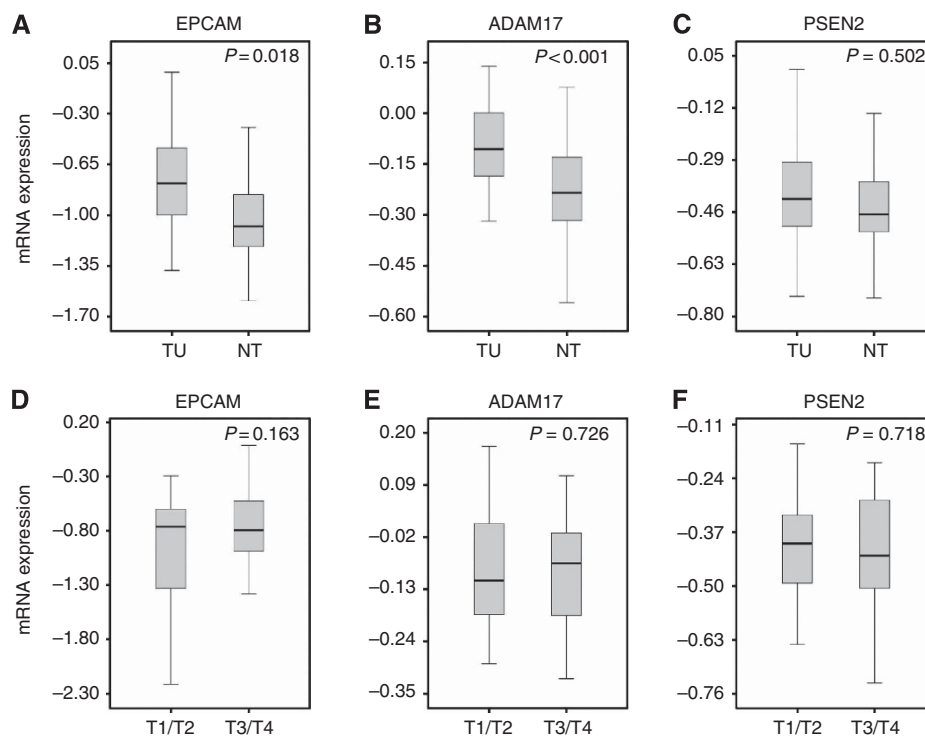


Figure 2. EPCAM, ADAM17, and PSEN2 expression in gastric tissue measured by real-time RT-PCR. Boxplots depicting mRNA levels of EPCAM (A and D; in 42 patients), ADAM17 (B and E; in 53 patients), and PSEN2 (C and F; in 54 patients). The upper panel depicts mRNA expression of EPCAM (A), ADAM17 (B), and PSEN2 (C) comparing malignant (TU) versus adjacent non-malignant (NT) gastric tissue. P -values were calculated with a paired two-sided Student's t -test. The lower panel shows mRNA expression of EPCAM (D), ADAM17 (E), and PSEN2 (F) comparing grouped T-categories. P -values were calculated with an unpaired two-sided Student's t -test.

t-test, got logarithmised to obtain approximately normally distributed data. A $P \leq 0.05$ was considered statistically significant. To account for the effects of multiple testing, we applied the explorative Simes (Benjamini–Hochberg) procedure within each group of tests (correlations and log-rank tests). The *P*-values are given unadjusted but are marked where they lose significance under the explorative Simes procedure (see Supplementary Table 2).

RESULTS

Study population. The clinico-pathological patient characteristics of the GC cohort are summarised in Table 1. Four hundred and eighty-two patients fulfilled all study criteria. According to Laurén, an intestinal-type GC was found in 240 (51.5%), a diffuse type in 146 (31.3%), a mixed type in 30 (6.4%), and an unclassifiable type in 50 (10.7%) patients. According to the mucin phenotype, 161 (39.0%) GCs were of the mixed, 122 (29.6%) of the intestinal, 68 (16.5%) of the unclassified and 61 (14.8%) of the gastric type (Supplementary Table 1).

Expression of EpCAM, PSEN2 and ADAM17 mRNA in GC. First we examined the transcriptional expression of *EPCAM*, *PSEN2*, and *ADAM17* in GC and corresponding non-neoplastic gastric mucosa. Real-time RT-PCR analysis was carried out on a series of 55 patients comprising malignant and corresponding non-malignant tissue, obtained from the same patients (Supplementary Table 2).

As shown in Figure 2, *EPCAM* and *ADAM17* mRNA levels were significantly increased in GC. However, no difference was found for *PSEN2* mRNA (Figure 2A–C).

Expression of members of the EpCAM signalling pathway on the translational level. Using immunohistochemistry and domain-specific antibodies directed against EpCAM, we next explored EpEX, EpICD, E-cadherin, β -catenin, PSEN2, and ADAM17 in GC (Figure 3) and non-neoplastic gastric mucosa (Figure 4).

Any immunolabelling of tumour cells for EpEX was found in 423 (90.8%) patients, for EpICD in 304 (67.6%), for E-cadherin in 407 (91.9%), for β -catenin in 429 (96.0%), for PSEN2 in 192 (49.4%), and for ADAM17 in 123 (27.0%) patients. Immunostaining of EpICD was further separated into membranous, cytoplasmic, or both, and was found in 223 (60.4%), 229 (61.1%), and 304 (67.6%) patients, respectively. The intensity of immunostaining varied for every member of the EpCAM signalling pathway between weak and strong immunolabelling. The amount of positive tumour cells varied between negative and abundant (>80% of the tumour cells). The distribution of the immunoreactivity scores (IRS) for each individual member is summarised in Table 2 and ranged between 0 and 8 for each antigen.

In non-neoplastic gastric mucosa, EpEX, EpICD, and ADAM17 were expressed only by single cells of the gastric pits commonly localised in the glands and never by the foveolar epithelium. Interestingly, PSEN2 was strongly expressed by the glandular epithelium and was undetectable in gastric foveolar epithelium (Figure 4). A strong membranous expression was found for E-cadherin and β -catenin in all types of gastric epithelial cells (Figure 4).

Statistical analyses. Next we correlated the expression of the diverse members of the EpCAM signalling pathway with various clinico-pathological patient characteristics. For this purpose, cases were divided into two groups (positive/negative) by splitting the immunoreactivity score at the median value, except for EpICD, where the distribution suggested splitting into score = 0 (negative) and score > 0 (positive; see Table 2). Following this dichotomisation, 134 (30.1%) tumours were categorised as positive for EpEX,

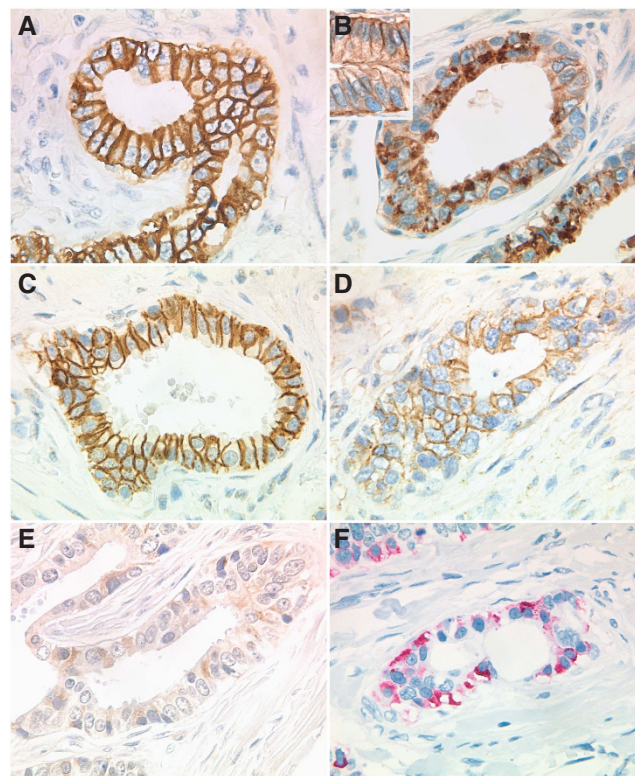


Figure 3. Detection of members of the EpCAM signalling pathway in GC tissue by immunohistochemistry. The expression of members of the EpCAM signalling pathway were explored by immunostaining using antibodies directed against EpEX (A), EpICD (B), β -catenin, (C) E-cadherin (D), PSEN2 (E), and ADAM17 (F). Note the membranous immunoreactions of EpEX (A), β -catenin (C), and E-cadherin (D), and the cytoplasmic immunoreactions of EpICD (B), PSEN2 (E), and ADAM17 (F). All pictures were taken from the same intestinal-type GC of a 47-year-old male patient. The insert in B illustrates membranous immunolabelling of EpICD in an intestinal-type GC of a different patient. Original magnifications, 600-fold.

223 (60.4%) for membranous EpICD, 229 (61.1%) for cytoplasmic EpICD, 304 (67.6%) for overall EpICD, 119 (26.9) for E-cadherin, 197 (44.1%) for β -catenin, 192 (49.4%) for PSEN2, and 123 (27.0%) for ADAM17 (Table 2).

Correlation of members of the EpCAM signalling pathway. First we tested the hypothesis, whether the expression of members of the EpCAM signalling pathway correlates with each other. As shown in Table 3, a significant coincidental expression was found for EpEX, EpICD, E-cadherin, β -catenin, PSEN2, and ADAM17. Only the expressions of ADAM17 and PSEN2, EpEX and PSEN2, and of E-cadherin and PSEN2 did not correlate with each other, respectively.

Supplementary Figure 2 summarises the similarities, differences, and relationships between the immunodetection of ADAM17, EpEX, and EpICD in the GC cohort.

Correlation with clinico-pathological patient characteristics. Next we tested the hypothesis that the expression of members of the EpCAM signalling pathway correlates with clinico-pathological patient characteristics (Supplementary Table 1).

The expression correlated significantly with tumour type according to Laurén (EpEX, EpICD-total, EpICD-membranous,

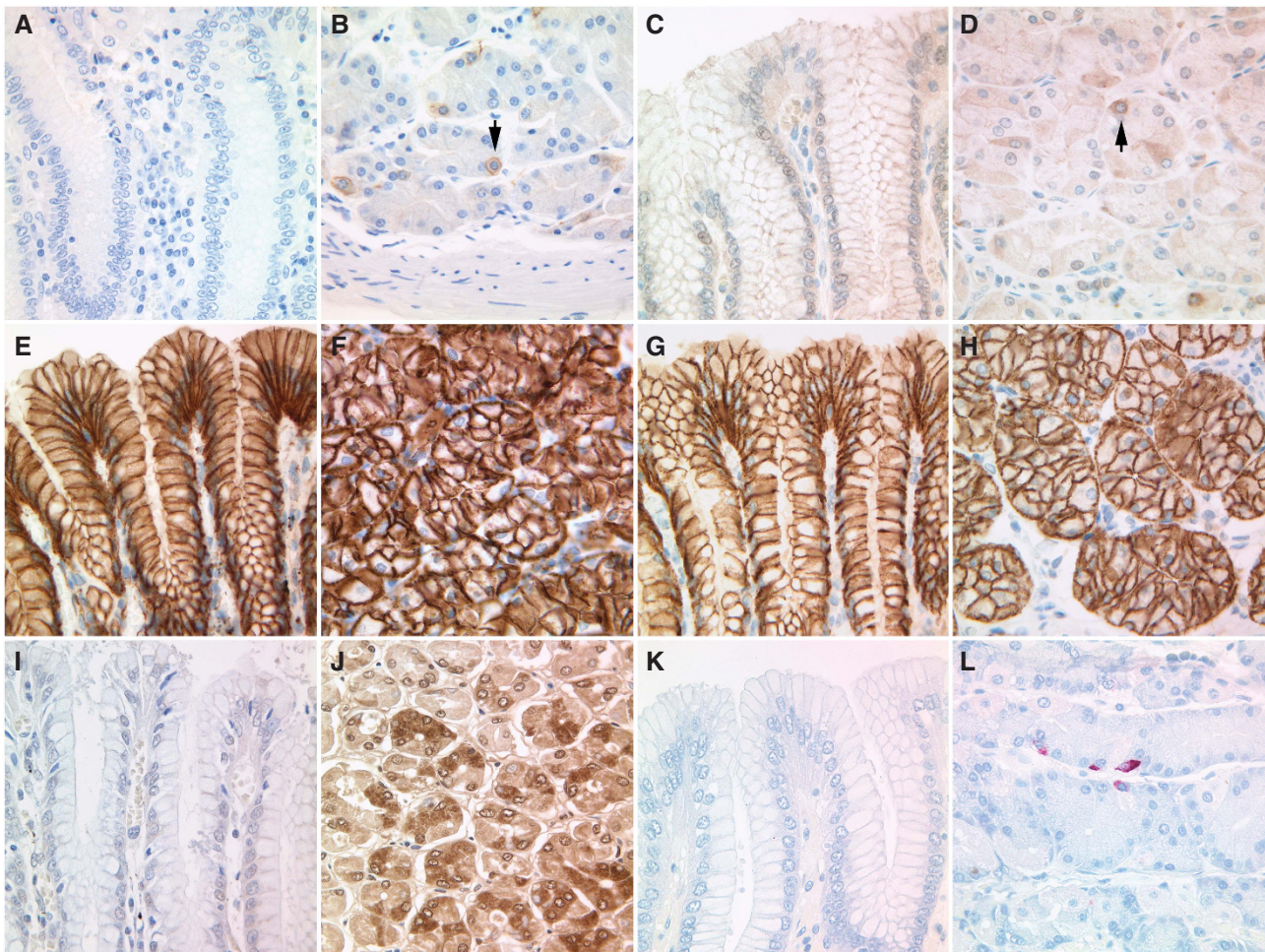


Figure 4. Detection of members of the EpCAM signalling pathway in non-neoplastic gastric mucosa by immunohistochemistry. The expression of members of the EpCAM signalling pathway were explored by immunostaining using antibodies directed against EpEX (**A** and **B**), EpICD (**C** and **D**), β -catenin (**E** and **F**), E-cadherin (**G** and **H**), PSEN2 (**I** and **J**), and ADAM17 (**K** and **L**). Note that EpEX, EpICD and ADAM17 were expressed only in few scattered cells of the gastric glands (**B**, **D**, and **L**; arrows) and absent in the foveolar epithelium (**A**, **C**, and **K**). β -catenin (**E** and **F**), and E-cadherin (**G** and **H**) were ubiquitously expressed. Interestingly, strong immunostaining was found for PSEN2 in gastric glands (**J**) and was completely absent in the gastric foveolar epithelium (**I**). Original magnifications, 400-fold.

EpICD-cytoplasmatic, E-cadherin, β -catenin, and PSEN2), mucin phenotype (EpEX, EpICD-total, EpICD-membranous, EpICD-cytoplasmatic, β -catenin, and ADAM17), T-category (EpEX, E-cadherin, and β -catenin), N-category (EpEX and β -catenin), UICC tumour stage (EpEX, EpICD-total, EpICD-cytoplasmatic, β -catenin, and PSEN2), tumour grade (EpEX, EpICD-total, EpICD-membranous, EpICD-cytoplasmatic, E-cadherin, β -catenin, and PSEN2), and patients' survival (EpEX, EpICD-cytoplasmatic, and PSEN2). For each member, the IRS decreased with increasing local tumour growth (T-category), nodal spread (N-category, lymph node ratio), tumour stage (UICC stage), and tumour grade. Thus, the overall immunodetection for the majority of members of the EpCAM signalling pathway (i.e., EpEX, EpICD, E-cadherin, β -catenin, and PSEN2) correlated inversely with local tumour growth, tumour stage, tumour grade, and, thus, the overall tumour progression.

In order to explore whether the shown dependency of the EpEX-IRS from local tumour growth (T-category) is a result of decreased transcription or protein degradation, we compared the ratio of EpCAM mRNA upregulation (i.e., the ratio of mRNA levels in tumour and non-tumour tissue for each case) with the local tumour growth (T-category). Because of the smaller number of cases in the subset, we divided the T-category into two groups,

that is, pT1/T2 and pT3/T4, and applied the two-sided Student's *t*-test. This showed no significant difference in EpCAM mRNA ratios between both groups ($P=0.163$; Figure 2D–F).

To confirm the dependence of EpEX-IRS (translational level) on pT-category in this small patient subset, we repeated Kendall's τ -test between the pT-category (grouped into pT1, pT2, pT3, and pT4) and EpEX status (negative or positive, dichotomised at the median IRS 7). This still showed a significant decrease of EpEX-IRS with increasing T-category ($P=0.023$). Thus, the decreased EpEX-IRS in GC is not linked to decreased gene transcription.

Prognostic markers of GC. Subsequently, we explored the prognostic significance of members of the EpCAM signalling pathway, using the log-rank test. Reduced immunodetection was associated with a significantly shorter patients' survival for EpEX (median 12.8 ± 1.2 months vs 18.0 ± 2.1 months; $P=0.010$), cytoplasmic EpICD (median 12.6 ± 1.5 months vs 18.2 ± 2.4 months; $P=0.013$), and PSEN2 (median 13.6 ± 1.5 months vs 16.0 ± 2.1 months; $P=0.019$). The Kaplan–Meier plots validated the significant correlation between EpEX, cytoplasmic EpICD, and PSEN2 detection and patients' survival (Figure 5).

Table 2. Distribution of the IRS and dichotomisation criteria

Marker	Distribution of IRS n (%)										Dichotomisation criteria and results	
	0	2	3	4	5	6	7	8	Median IRS	Neg. (n (%))	Pos. (n (%))	
EpEX (BerEP4)	22 (4.9)	9 (2.0)	15 (3.4)	29 (6.5)	51 (11.5)	72 (16.2)	113 (25.4)	134 (30.1)	7	IRS ≤ 7 311 (69.9)	IRS > 7 134 (30.1)	
EpICD-membranous	146 (39.6)	2 (0.5)	17 (4.6)	36 (9.8)	50 (13.6)	55 (14.9)	41 (11.1)	22 (6.0)	4	IRS = 0 146 (39.6)	IRS > 0 223 (60.4)	
EpICD-cytoplasmatic	146 (38.9)	14 (3.7)	26 (6.9)	39 (10.4)	59 (15.7)	42 (11.2)	36 (9.6)	13 (3.5)	4	IRS = 0 146 (38.9)	IRS > 0 229 (61.1)	
EpICD-overall	146 (32.4)	14 (3.1)	34 (7.6)	53 (11.8)	71 (15.8)	64 (14.2)	46 (10.2)	22 (4.9)	4	IRS = 0 146 (32.4)	IRS > 0 304 (67.6)	
E-cadherin	36 (8.1)	4 (0.9)	11 (2.5)	13 (2.9)	54 (12.2)	85 (19.2)	121 (27.3)	119 (26.9)	7	IRS < 7 324 (73.1)	IRS > 7 119 (26.9)	
β-catenin	18 (4.0)	6 (1.3)	20 (4.5)	29 (6.5)	83 (18.6)	94 (21.0)	105 (23.5)	92 (20.6)	6	IRS ≤ 6 250 (55.9)	IRS > 6 197 (44.1)	

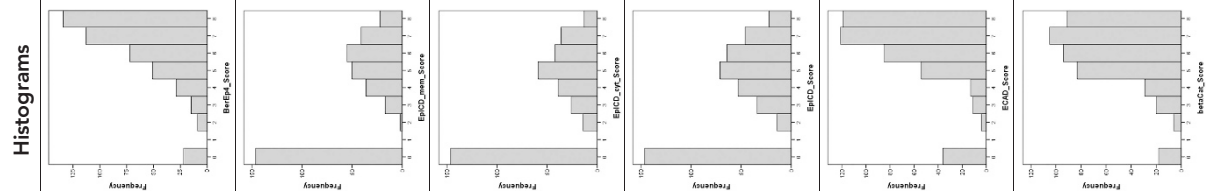


Table 2. (Continued)

Marker	Valid n (%)	Missing n (%)	Histograms	Distribution of IRS n (%)								Dichotomisation criteria and results			
				0	2	3	4	5	6	7	8	Median IRS	Neg. (n (%))	Pos. (n (%))	
Presenilin 2	389 (80.7)	93 (19.3)		197 (50.6)	10 (2.6)	29 (7.5)	38 (9.8)	38 (9.8)	38 (9.8)	23 (5.9)	37 (9.5)	17 (4.4)	0	IRS = 0 197 (50.6)	IRS > 0 192 (49.4)
ADAM17	455 (94.4)	27 (5.6)		332 (73.0)	4 (0.9)	8 (1.8)	62 (13.6)	37 (8.1)	10 (2.2)	2 (0.4)	0 (0.0)	0	IRS = 0 332 (73.0)	IRS > 0 123 (27.0)	

Abbreviations: EpCAM = epithelial cell adhesion molecule; EpEX = extracellular domain of EpCAM; EpICD = intracellular domain of EpCAM; IRS = immunoreactivity scores; Neg. = negative; Pos. = positive. Where the IRS distribution clearly showed two distinct features, we used these to divide into negative and positive cases (EpICD, IRS = 0 as negative and IRS > 0 as positive). Where no such distinction was possible, we used the median of the IRS to divide into negative and positive groups. Dichotomisation criteria are listed in the last column.

In addition, patient prognosis significantly depended on Laurén-phenotype, tumour grade, T-category, N-category, LNR, R-status, as well as UICC stage and ‘Kiel stage’ (data not shown).

Multivariate survival analysis (Cox regression). A Cox regression was carried out on all parameters, which had a $P < 0.10$ in univariate survival analysis, that is, age group, Laurén phenotype, T-category, N-category, UICC stage, stage according to the ‘Kiel proposal’ (Warneke *et al*, 2011), lymph node ratio, grading, resection margin, EpEX expression, EpICD expression (total, membranous, and cytoplasmatic), and PSEN2 expression. The parameters that remain in the Cox model after running the backward LR method with $P_{in} = 0.05$ and $P_{out} = 0.10$ were resection margin (HR 1.700 (95% CI 1.045–2.765); $P = 0.033$), age group (1.586 (1.154–2.179); $P = 0.004$), lymph node ratio (1.476 (0.970–2.247); $P = 0.069$), and stage according to the ‘Kiel proposal’ (1.078 (1.047–1.110); $P < 0.001$). Although the aforementioned biomarkers show prognostic value in univariate analysis, the independence of their prognostic value cannot be confirmed in multivariate analysis.

DISCUSSION

EpCAM (CD326) is a calcium-independent type I transmembrane glycoprotein of 314 amino acids with a molecular weight of ~39–42 kDa. EpCAM consists of extracellular EGF-like and thyroglobulin repeat domains, a single-spanning transmembrane domain, and an intracellular domain of 26 amino acids containing an NPCY-internalisation motif and two binding sites for α -catenin (Figure 1; Baeuerle and Gires, 2007; Trzpis *et al*, 2007; Munz *et al*, 2009). EpCAM is present in embryonic stem cells that are not yet committed to the epithelial cell type during embryonal development, is expressed in most normal epithelia on the basolateral cell surface, and is upregulated on most human adenocarcinomas as well as squamous cell carcinomas (Patriarca *et al*, 2012). It is one of the most frequently and most intensely expressed tumour-associated antigens currently known (Baeuerle and Gires, 2007; Trzpis *et al*, 2007; Munz *et al*, 2009; Patriarca *et al*, 2012). BerEP4-antibody-labelled magnetic Dynabeads, targeting the EpEX, are used to separate epithelial from non-epithelial cells in tissue homogenates (Ebert *et al*, 2005).

Although EpCAM was initially thought to function as a homotypic intercellular adhesion molecule (Litvinov *et al*, 1994), evidence is increasing that EpCAM is also a receptor involved in the regulation of gene transcription and cell proliferation. Overexpression of EpCAM in cancer cells is linked to tumour cell differentiation, migration, and proliferation. It stimulates the cell cycle by upregulating *c-myc* and cyclins (Baeuerle and Gires, 2007; Trzpis *et al*, 2007; Munz *et al*, 2009; Patriarca *et al*, 2012). Maetzel *et al* (2009) recently provided evidence that EpCAM may mediate these diverse cancer biological functions, after intramembrane proteolysis by two distinct proteases (i.e., ADAM17 and PSEN2) has liberated the intracellular domain EpICD, which then forms a nuclear protein complex, leading to gene transcription (Figure 1). In our retrospective observational study, we provide evidence that diverse members of the EpCAM signalling pathway are expressed in GC and are of putative tumour biological significance. EpCAM expression has divergent prognostic affects: in some tumour types a negative correlation was found, in most a seemingly neutral effect, and in some cancer types a positive correlation was found (Baeuerle and Gires, 2007). In this respect, it was interestingly to note that EpCAM was present only in single cells of the non-neoplastic mucosa and was significantly upregulated on the transcriptional and translational level in GC. This finding supports

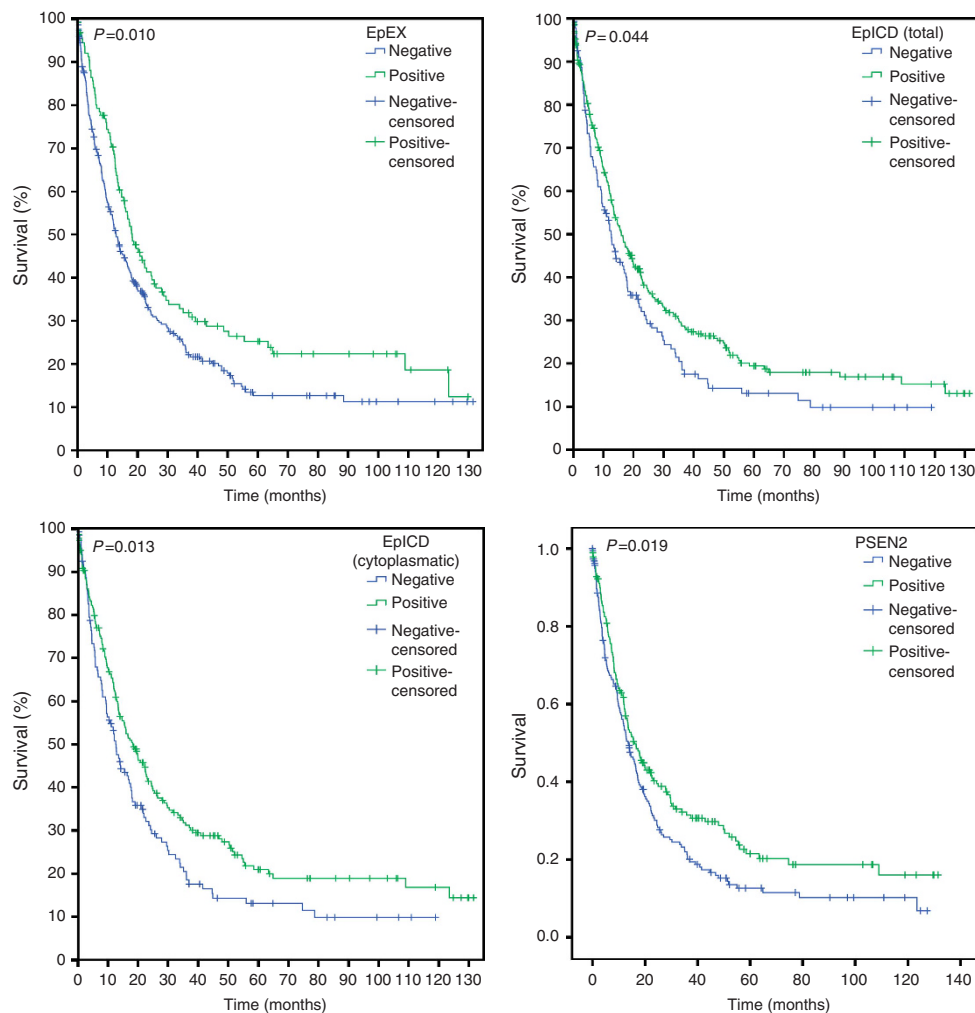


Figure 5. Patients' survival. Kaplan–Meier curves depicting patients' survival according to immunodetection of EpEX (all cases, $P=0.010$), EpICD-total (all cases; $P=0.044$), EpICD cytoplasmic (all cases, $P=0.013$), and PSEN2 (all cases, $P=0.019$).

the conjecture that EpCAM is of relevance in tumour cell biology. Further progression with regard to local tumour growth, nodal spread, and overall tumour stage was associated with a significantly reduced immunodetection of EpCAM (and also of E-cadherin and β -catenin). These findings are in line with those published by Songun *et al* (2005), who have shown that reduced detection of EpCAM is associated with a significantly worse prognosis. Thus, immunodetection of EpCAM in GC seemingly appears to be associated with a more favorable prognosis. However, Maetzel *et al* (2009) have shown that EpCAM is prone to RIP and, apart from reduced transcription, increased proteolysis may also contribute to reduced immunodetection. In our study we provide circumstantial evidence that RIP of EpCAM may take place in GC:

(1) We confirm independently the differential expression of ADAM17 in GC cells, which has been previously shown by us and others (Schmuck *et al*, 2011; Shou *et al*, 2012; Zhang *et al*, 2012). Overexpression of ADAM17 may be a further means to control and promote EpCAM signalling (Munz *et al*, 2009).

(2) We believe that we are the first to demonstrate the expression of PSEN2 in GC tissue samples, which may release EpICD through γ -secretase intramembrane-cleaving activity in GC (Maetzel *et al*, 2009). In this respect, it was also interesting to note that the immunodetection of PSEN2 did not correlate with EpEX but with EpICD, lending further support to our hypothesis.

Proteolysis of EpCAM by PSEN2 may liberate the intracellular domain detected by EpICD (see Figure 1).

(3) Using domain-specific antibodies, we were able to show that epitopes of EpCAM are not only found at the cell membrane but also in the cytoplasm.

(4) Finally, we show that the decreased immunodetection of EpEX in locally advanced GC is not accompanied by decreased EpCAM mRNA levels. The latter finding support our hypothesis of proteolytic cleavage of EpCAM in GC.

There have been a variety of reports about the interaction between EpCAM, members of the EpCAM signalling pathway, and molecules of the WNT pathway. The function of EpCAM in cell adhesion is interconnected with E-cadherin (Litvinov *et al*, 1997). By the upregulation of EpCAM, E-cadherin-mediated cell adhesion diminishes and the EpCAM-mediated adhesion may predominate (Went *et al*, 2006). This might explain that EpCAM (EpEX and EpICD)-positive cancers were between 1.3- and 2.1-fold, more commonly negative than positive for E-cadherin in our cohort (Table 3). PSENs, in turn, regulate β -catenin stability (Nishimura *et al*, 1999; Brunkan and Goate, 2005), which may explain the significant positive correlation between PSEN2 and β -catenin expression in our patient cohort. Thus, our study supports the notion that the EpCAM signalling pathway is involved in GC biology, and RIP merits further attention and, in depth, functional studies in GC.

Table 3. Coincidental expression of members of the EpCAM signalling pathway in GC tissue

	ADAM17		Presenilin 2		β -catenin		E-cadherin		EpICD-total		EpICD-cytoplasmatic		EpICD-membranous	
	Negative (n (%))	Positive (n (%))	Negative (n (%))	Positive (n (%))	Negative (n (%))	Positive (n (%))	Negative (n (%))	Positive (n (%))	Negative (n (%))	Positive (n (%))	Negative (n (%))	Positive (n (%))	Negative (n (%))	Positive (n (%))
All patients														
EpEX	n=431 $\tau=0.179$	P<0.001	n=374 $\tau=0.087$	P=0.301 R(t)=0.035	n=427 $\tau=0.037$	P<0.001	n=429 $\tau=0.036$	P<0.001	n=430 $\tau=0.034$	P<0.001	n=355 $\tau=0.370$	P<0.001	n=352 $\tau=0.421$	P<0.001
Negative	236 (54.8)	67 (15.5)	140 (37.4)	129 (34.5)	182 (42.6)	116 (27.2)	238 (55.5)	63 (14.7)	120 (27.9)	183 (42.6)	120 (33.8)	140 (39.4)	120 (34.1)	119 (33.8)
Positive	75 (17.4)	53 (12.3)	48 (12.8)	57 (15.2)	53 (12.4)	76 (17.8)	73 (17.0)	55 (12.8)	13 (3.0)	114 (26.5)	13 (3.7)	82 (23.1)	13 (3.7)	100 (28.4)
EpICD-membranous														
Negative	n=359 $\tau=0.156$	P=0.007 P(t)=0.001	n=310 $\tau=0.223$	P=0.001	n=360 $\tau=0.290$	P<0.001	n=356 $\tau=0.253$	P<0.001	n=369 $\tau=1.000$	P<0.001	n=294 $\tau=1.000$	P<0.001		
Positive	113 (31.5)	25 (7.0)	75 (24.2)	45 (14.5)	101 (28.1)	38 (10.6)	114 (32.0)	23 (6.5)	146 (39.6)	0 (0.0)	146 (49.7)	0 (0.0)		
EpICD-cytoplasmatic														
Negative	n=364 $\tau=0.151$	P=0.005 P(t)=0.001	n=323 $\tau=0.243$	P<0.001	n=363 $\tau=0.256$	P<0.001	n=362 $\tau=0.281$	P<0.001	n=375 $\tau=1.000$	P<0.001	n=294 $\tau=1.000$	P<0.001		
Positive	113 (31.0)	25 (6.9)	75 (23.2)	45 (13.9)	101 (27.8)	38 (10.5)	114 (31.5)	23 (6.4)	146 (38.9)	0 (0.0)	146 (49.7)	0 (0.0)		
EpICD-total														
Negative	n=439 $\tau=0.128$	P=0.004 P(t)=0.004	n=381 $\tau=0.219$	P=0.002 R(t)<0.001	n=438 $\tau=0.265$	P<0.001	n=435 $\tau=0.235$	P<0.001	n=435 $\tau=0.235$	P<0.001				
Positive	113 (25.7)	25 (5.7)	75 (19.7)	45 (11.8)	101 (23.1)	38 (8.7)	114 (26.2)	23 (5.3)	146 (32.8)	0 (0.0)	146 (38.9)	0 (0.0)		
E-cadherin														
Negative	n=432 $\tau=0.102$	P=0.021 P(t)=0.014	n=377 $\tau=0.073$	P=0.116 R(t)=0.078	n=434 $\tau=0.331$	P<0.001	n=434 $\tau=0.331$	P<0.001	n=438 $\tau=0.265$	P<0.001				
Positive	207 (47.2)	94 (21.4)	118 (31.0)	143 (37.5)	143 (32.6)	156 (35.6)	202 (46.4)	96 (22.1)	119 (27.2)	223 (60.4)	0 (0.0)	148 (50.3)		
β-catenin														
Negative	n=435 $\tau=0.087$	P=0.017 P(t)=0.034	n=375 $\tau=0.224$	P<0.001	n=434 $\tau=0.331$	P<0.001	n=434 $\tau=0.331$	P<0.001	n=438 $\tau=0.265$	P<0.001				
Positive	73 (16.9)	42 (9.7)	50 (13.3)	64 (17.0)	41 (9.4)	75 (17.3)								
Presenilin 2														
Negative	n=383 $\tau=0.070$	P=0.491 P(t)=0.114	n=375 $\tau=0.224$	P<0.001	n=434 $\tau=0.331$	P<0.001	n=434 $\tau=0.331$	P<0.001	n=438 $\tau=0.265$	P<0.001				
Positive	186 (42.8)	55 (12.6)	121 (32.3)	85 (22.7)	121 (32.3)	85 (22.7)								
ADAM17														
Negative	n=383 $\tau=0.070$	P=0.491 P(t)=0.114	n=375 $\tau=0.224$	P<0.001	n=434 $\tau=0.331$	P<0.001	n=434 $\tau=0.331$	P<0.001	n=438 $\tau=0.265$	P<0.001				
Positive	146 (38.1)	50 (13.1)	67 (17.9)	102 (27.2)										
Presenilin 2														
Negative	n=383 $\tau=0.070$	P=0.491 P(t)=0.114	n=375 $\tau=0.224$	P<0.001	n=434 $\tau=0.331$	P<0.001	n=434 $\tau=0.331$	P<0.001	n=438 $\tau=0.265$	P<0.001				
Positive	146 (38.1)	50 (13.1)	67 (17.9)	102 (27.2)										
EpCAM														
Negative	n=383 $\tau=0.070$	P=0.491 P(t)=0.114	n=375 $\tau=0.224$	P<0.001	n=434 $\tau=0.331$	P<0.001	n=434 $\tau=0.331$	P<0.001	n=438 $\tau=0.265$	P<0.001				
Positive	146 (38.1)	50 (13.1)	67 (17.9)	102 (27.2)										

Abbreviations: EpCAM = epithelial cell adhesion molecule; EpEX = extracellular domain of EpCAM; EpICD = intracellular domain of EpCAM; GC = gastric cancer; τ denotes Kendall's τ ; τ ranges from -1 (maximally negative correlation) to +1 (maximally positive correlation). P denotes P-value of Fisher's exact test. R(t) denotes Kendall's τ , if it is different from P.

ACKNOWLEDGEMENTS

CR is supported by grants of the Deutsche Forschungsgemeinschaft (Grant-No. Ro 1173/11 and Ro 1173/12).

CONFLICT OF INTEREST

The authors declare no conflict of interests.

REFERENCES

- Alberts SR, Cervantes A, van de Velde CJ (2003) Gastric cancer: epidemiology, pathology and treatment. *Ann Oncol* **14**(Suppl 2): ii31–ii36.
- Baeuerle PA, Gires O (2007) EpCAM (CD326) finding its role in cancer. *Br J Cancer* **96**(3): 417–423.
- Brunkan AL, Goate AM (2005) Presenilin function and gamma-secretase activity. *J Neurochem* **93**(4): 769–792.
- Buhard O, Cattaneo F, Wong YF, Yim SF, Friedman E, Flejou JF, Duval A, Hamelin R (2006) Multipopulation analysis of polymorphisms in five mononucleotide repeats used to determine the microsatellite instability status of human tumors. *J Clin Oncol* **24**(2): 241–251.
- Campbell WA, Iskandar MK, Reed ML, Xia W (2002) Endoproteolysis of presenilin in vitro: inhibition by gamma-secretase inhibitors. *Biochemistry* **41**(10): 3372–3379.
- Cunningham D, Allum WH, Stenning SP, Thompson JN, van de Velde CJ, Nicolson M, Scarffe JH, Lofts FJ, Falk SJ, Iveson TJ, Smith DB, Langley RE, Verma M, Weeden S, Chua YJ, MAGIC TP (2006) Perioperative chemotherapy versus surgery alone for resectable gastroesophageal cancer. *N Engl J Med* **355**(1): 11–20.
- Ebert MP, Krüger S, Fogeron ML, Lamer S, Chen J, Pross M, Schulz HU, Lage H, Heim S, Roessner A, Malfertheiner P, Röcken C (2005) Overexpression of cathepsin B in gastric cancer identified by proteome analysis. *Proteomics* **5**(6): 1693–1704.
- Lauren T (1965) The two histologic main types of gastric carcinoma: Diffuse and so-called intestinal-type carcinoma. *Acta Pathol Microbiol Scand* **64**: 31–49.
- Litvinov SV, Balzar M, Winter MJ, Bakker HA, Briaire-de Bruijn IH, Prins F, Fleuren GJ, Warnaar SO (1997) Epithelial cell adhesion molecule (Ep-CAM) modulates cell-cell interactions mediated by classic cadherins. *J Cell Biol* **139**(5): 1337–1348.
- Litvinov SV, Velders MP, Bakker HA, Fleuren GJ, Warnaar SO (1994) Ep-CAM: a human epithelial antigen is a homophilic cell-cell adhesion molecule. *J Cell Biol* **125**(2): 437–446.
- Maetzel D, Denzel S, Mack B, Canis M, Went P, Benk M, Kieu C, Papior P, Baeuerle PA, Munz M, Gires O (2009) Nuclear signalling by tumour-associated antigen EpCAM. *Nat Cell Biol* **11**(2): 162–171.
- Munz M, Baeuerle PA, Gires O (2009) The emerging role of EpCAM in cancer and stem cell signaling. *Cancer Res* **69**(14): 5627–5629.
- Namikawa T, Hanazaki K (2010) Mucin phenotype of gastric cancer and clinicopathology of gastric-type differentiated adenocarcinoma. *World J Gastroenterol* **16**(37): 4634–4639.
- Nishimura M, Yu G, Levesque G, Zhang DM, Ruel L, Chen F, Milman P, Holmes E, Liang Y, Kawarai T, Jo E, Supala A, Rogaeva E, Xu DM, Janus C, Levesque L, Bi Q, Duthie M, Rozmahel R, Mattila K, Lannfelt L, Westaway D, Mount HT, Woodgett J, St George-Hyslop P (1999) Presenilin mutations associated with Alzheimer disease cause defective intracellular trafficking of beta-catenin, a component of the presenilin protein complex. *Nat Med* **5**(2): 164–169.
- Paoletti X, Oba K, Burzykowski T, Michiels S, Ohashi Y, Pignon JP, Rougier P, Sakamoto J, Sargent D, Sasako M, Van CE, Buyse M (2010) Benefit of adjuvant chemotherapy for resectable gastric cancer: a meta-analysis. *JAMA* **303**(17): 1729–1737.
- Patriarca C, Macchi RM, Marschner AK, Mellstedt H (2012) Epithelial cell adhesion molecule expression (CD326) in cancer: a short review. *Cancer Treat Rev* **38**(1): 68–75.
- Schmuck R, Warneke V, Behrens HM, Simon E, Weichert W, Röcken C (2011) Genotypic and phenotypic characterization of side population of gastric cancer cell lines. *Am J Pathol* **178**(4): 1792–1804.
- Shou ZX, Jin X, Zhao ZS (2012) Upregulated expression of ADAM17 is a prognostic marker for patients with gastric cancer. *Ann Surg* **256**(6): 1014–1022.
- Sobin LH, Gospodarowicz M, Wittekind C (2009) *TNM Classification of Malignant Tumours*. Wiley-Blackwell.
- Songun I, Litvinov SV, van de Velde CJ, Pals ST, Hermans J, van Krieken JH (2005) Loss of Ep-CAM (CO17-1A) expression predicts survival in patients with gastric cancer. *Br J Cancer* **92**(9): 1767–1772.
- Trzpis M, McLaughlin PM, de Leij LM, Harmsen MC (2007) Epithelial cell adhesion molecule: more than a carcinoma marker and adhesion molecule. *Am J Pathol* **171**(2): 386–395.
- van Dongen JJ, Langerak AW, Bruggemann M, Evans PA, Hummel M, Lavender FL, Delabesse E, Davi F, Schuurung E, Garcia-Sanz R, van Krieken JH, Droese J, Gonzalez D, Bastard C, White HE, Spaargaren M, Gonzalez M, Parreira A, Smith JL, Morgan GJ, Kneba M, Macintyre EA (2003) Design and standardization of PCR primers and protocols for detection of clonal immunoglobulin and T-cell receptor gene recombinations in suspect lymphoproliferations: report of the BIOMED-2 Concerted Action BMH4-CT98-3936. *Leukemia* **17**(12): 2257–2317.
- Walter J, Grünberg J, Schindzielorz A, Haass C (1998) Proteolytic fragments of the Alzheimer's disease associated presenilins-1 and -2 are phosphorylated in vivo by distinct cellular mechanisms. *Biochemistry* **37**(17): 5961–5967.
- Warneke VS, Behrens HM, Hartmann JT, Held H, Becker T, Schwarz NT, Röcken C (2011) Cohort study based on the seventh edition of the TNM classification for gastric cancer: proposal of a new staging system. *J Clin Oncol* **29**(17): 2364–2371.
- Weichert W, Röske A, Gekeler V, Beckers T, Ebert MP, Pross M, Dietel M, Denkert C, Röcken C (2008) Association of patterns of class I histone deacetylase expression with patient prognosis in gastric cancer: a retrospective analysis. *Lancet Oncol* **9**(2): 139–148.
- Went P, Vasei M, Bubendorf L, Terracciano L, Tornillo L, Riede U, Kononen J, Simon R, Sauter G, Baeuerle PA (2006) Frequent high-level expression of the immunotherapeutic target Ep-CAM in colon, stomach, prostate and lung cancers. *Br J Cancer* **94**(1): 128–135.
- Zhang TC, Zhu WG, Huang MD, Fan RH, Chen XF (2012) Prognostic value of ADAM17 in human gastric cancer. *Med Oncol* **29**(4): 2684–2690.

This work is published under the standard license to publish agreement. After 12 months the work will become freely available and the license terms will switch to a Creative Commons Attribution-NonCommercial-Share Alike 3.0 Unported License.

Supplementary Information accompanies this paper on *British Journal of Cancer* website (<http://www.nature.com/bjc>)